Learn low wavenumber information in FWI via Deep Inception based Convolutional Networks

Yuchen Jin, University of Houston, Wenyi Hu†, Advanced Geophysical Technology Inc., Xuqing Wu*, and Jiefu Chen*, University of Houston*

SUMMARY

In this paper, we will explore the possibility of synthesizing the low-frequency data from the high-frequency data and use the predicted result to improve the full-waveform inversion (FWI). Unlike all previously methods, to the best of our knowledge, this is the first attempt to utilize a data driven approach to solve the problem. We have proposed to learn the low wavenumber information in FWI via the Deep Inception based Convolutional Networks. Once the deep learning model is sufficiently trained, the model can be used to predicted the low-frequency data with high accuracy on a completely different velocity model. In the end, we validate the quality of the predicted low-frequency data and the robustness of this deep learning approach.

INTRODUCTION

In current seismic data acquisition environments, reliable low-frequency components below 5 Hz do not practically exist in typical seismic data sets. This will affect the performance of FWI, which takes into account the full waveform information of seismic data to reconstruct an earth model and is expected to generate the maps of geophysical properties continuously covering a broadband wavenumber spectrum. Without low-wavenumber components of the velocity model, FWI may converge to a local minimum when the inversion starts at high frequencies or the starting velocity model is not sufficiently close to the true model. Computationally synthesizing the low frequencies from the high-frequency data has attracted much attention recently. However, it is a very challenging signal-processing problem and is a highly nonlinear operation. This paper will be kept brief with regard to the treatment of related research works. Readers who are interested in more technical aspects of this topic can refer to articles such as Ma and Hale (2013), Baek et al. (2014), Warner and Guasch (2016), Van Leeuwen and Herrmann (2013), Tang et al. (2013), Alkhalifah (2014), and Li and Demanet (2016). The review articles published by Hu et al. (2018) provides a comprehensive overview of latest research advances.

Following a phase modulation/demodulation concept commonly used by musicians for instrument tuning, Hu (2014) proposed beat tone FWI to suppress the cycle-skipping phenomenon. This method utilizes two seismic data sets at two slightly different high frequencies to infer the data set at a low frequency. However, although the beat tone strategy successfully amplifies the low wavenumber information, it fails to completely exclude the information of the high wavenumber. Figure 1 show the comparison between ground-truth 3 [Hz] data and the beat tone data extracted from the 8 [Hz] and 11 [Hz] data.

By observing the behavior of the beat tone data, we found

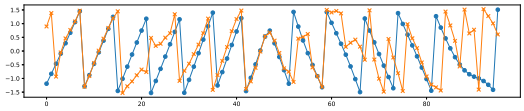

Figure 1: An example data generated on a Marmousi model. The blue line represents the true 3 [Hz] data. The orangle line indicates beat tone data extracted from the 8 [Hz] and 11 [Hz] data.

that the naive regression model is unable to find a reliable method that could synthesize the data of low frequencies from the high-frequency data. However, we hypothesize that, first, a mapping function exists for a given subsurface structure. Second, we could find a robust mapping function that adapts to different subsurface structures by mining the relationship via a data drive approach. In this paper, we propose a novel data driven framework and verify its feasibility in synthesizing the low-frequency data from the high-frequency data. Our method is built upon a deep inception based convolutional network (Szegedy et al. (2015)) and its structural detail will be explained in the following sections.

A DATA DRIVEN FRAMEWORK FOR LEARNING LOW-FREQUENCY DATA FROM HIGH-FREQUENCY DATA

Figure 2 shows that our framework is divided into two phases. In the first phase, we preprocess the high-frequency data in the complex domain. In the second phase, the processed data will be fed into the deep nural network to predict the corresponding low-frequency data.

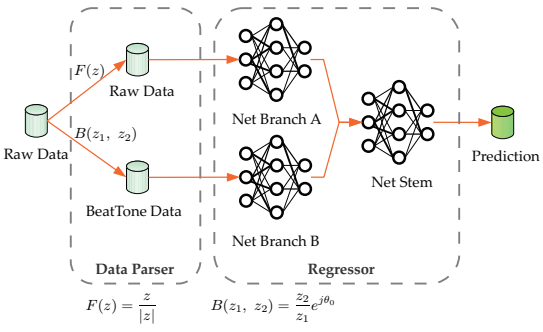

Figure 2: The structure of the data driven frame for learning the low-frequency data.

Data Preprocessing

The model will be trained with two kinds of data:

(1) **Normalized raw data**: The amplitude of the raw data is normalized in the complex domain, this operator can be desribed as $F(z) = \frac{z}{|z|}$;

(2) **Beat tone data**: The beat tone data is generated according to Hu (2014). Denote two high frequency-data z_1 and z_2 with frequencies respectively at f_1 and f_2 ($f_2 > f_1$), the beat tone data is generated as $B(z_1, z_2) = \frac{z_2}{z_1} e^{j\theta_0}$, and the beat tone frequency will be $f_2 - f_1$.

The real part and the imaginary part of the data at different frequencies will be fed into different channels of the convolutional network. For data collected at consecutive frequencies $\{f_l,\ f_l + \Delta f,\ f_l + 2\Delta f,\ \ldots,\ f_h\}$, the number of channels required for the normalized raw data is:

$$C_r = 2 \cdot \left(\frac{f_h - f_l}{\Delta f} + 1 \right). \tag{1}$$

To generate the beat tone data for a specified low-frequency at f_o, we need two data sets of high-frequencies at $(f, f + f_o)$. The network can be trained to synthesize data at multiple low-frequencies. Using N as the number of total low-frequency data sets the network can produce, the number of input channels required by the beat tone data is:

$$C_b = 2 \cdot \sum_{i=0}^{N-1} \left(\frac{f_h - f_o^{(i)} - f_l}{\Delta f} + 1 \right). \tag{2}$$

Then the number of channels of the network output is:

$$C_o = 2N. \tag{3}$$

In the experiments, we use $8 \leqslant f \leqslant 18$ [Hz] data to predict $\{1.5,\ 3,\ 5\}$ [Hz] data and $10 \leqslant f \leqslant 18$ [Hz] data to predict $\{1.5,\ 3,\ 5,\ 7\}$ [Hz] data. The channel numbers in our experiment are summarized in Table 1 and $\Delta f = 0.5$ [Hz].

Input Band	C_r	C_b	C_o
$\geqslant 8$ [Hz]	42	88	6
$\geqslant 10$ [Hz]	34	70	8

Table 1: Channel numbers in experiments

Deep Inception based Convolutional Networks

As shown in Figure 2, any arbitrary neural network could be used in the framework. We have designed and tested with different network structures. The framework learns to synthesize the low-frequency data by using both the normalized high-frequency data and the beat tone data. Therefore, the network is set to learn a model that will amplify the low wavenumber information and exclude the high wavenumber information at the same time. The branch A and B share the same structure. Their outputs would be merged together by the channel concatenation. The merged layer would be fed into a stem network with mixed features from both branches and the output is mapped to the low-frequency data.

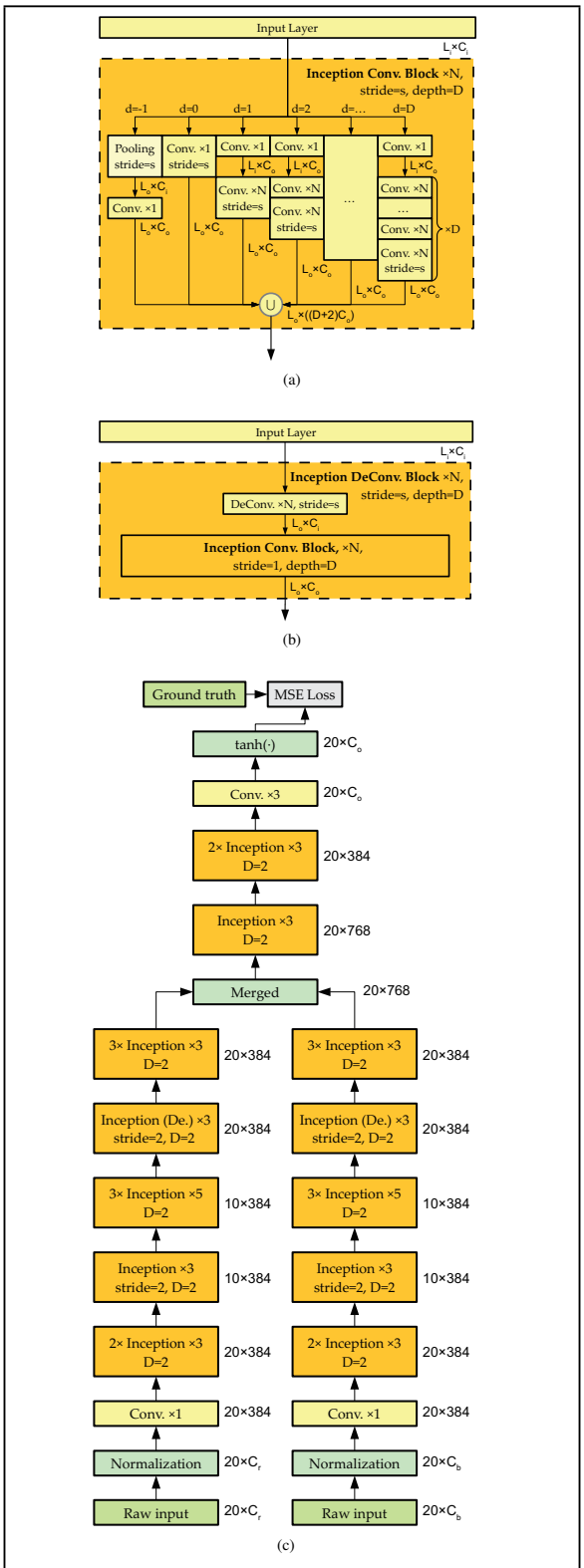

Figure 3: The structures of basic units of D-depth inception model.

Among all networks we have tested so far, the inception based convolutional network (Szegedy et al. (2017)) is most effective in solving the problem. Figure 3a and Figure 3b shows the two basic units of the inception model. Figure 3a shows the convolutional block which is composes of $D+2$ parallel branches. Denote the depth as d, then:

(1) If $d=-1$, this branch has a pooling layer and a $\times 1$ convolutional layer (which is also called projection).

(2) If $d=0$, this branch only has a projection layer, which means it is just a combination of the original features.

(3) If $d>0$, there would be d convolutional layers after the projection. The projection will produce an output with the length of $2\times(d-1)\times\lfloor\frac{N}{2}\rfloor+N$.

The cup sign ($\bigcup$) in Figure 3a represents concatenating all channels from each branches. Since there are $D+2$ branches, if each branch has C_o output channels, the number of output channels of the whole block will be $(D+2)C_o$. The other basic unit is the deconvolutinal block which is illustrated in Figure 3b. It is designed by adding a deconvolutional layer before the convolutional inception block. The deconvlutional layer will up-sample the input layers by the stride of s. In the regression model we may need to reduce the length of the sample during the convolution and use this operation to recover the original length so that the features would be easier to be mapped to the target space.

Figure 3c shows the structure of the regressor. We crop several samples with a length of 20 from the original 96-length samples randomly. Then the samples could be pre-processed for the raw data and beat tone data respectively. In each branch network we use 10 inception block and concatenate the output channels from 2 branch networks. In Figure 3c, all depths (denoted as D) of every individual inception block is set to be 2. The depth of the whole network is 41. We use tanh function to map the output to the range of $(-1,\ 1)$. The objective of the learning process is to minimize the MSE loss against the ground truth. The network can be represented as a function $\mathscr{F}(\mathbf{x},\ \mathbf{\Theta})$, where $\mathbf{x}$ represents the input, $\mathbf{\Theta}$ are all parameters of the network. Given the ground truth $\mathbf{y}$, the optimization can be described as:

$$\min_{\mathbf{\Theta}}\sum_{\mathbf{x},\mathbf{y}}\|\mathscr{F}(\mathbf{x},\ \mathbf{\Theta})-\mathbf{y}\|_2^2. \tag{4}$$

FEASIBILITY STUDY

In order to verify the robustness of the model for adapting to different subsurface structures, *the Deep Inception based Convolutional Networks are trained with SEG Model 1997 2.5D and tested against the Marmousi Model*. Figure 4 shows the training and validation accuracy when using different sets of high-frequency data. It indicates that as the frequency gets higher, the accuracy for predicting low-frequency data is getting lower.

Figure 5a show the true 3 [Hz] Marmousi data (blue) and the beat tone 3 [Hz] data (orange) extracted from 13 [Hz] and

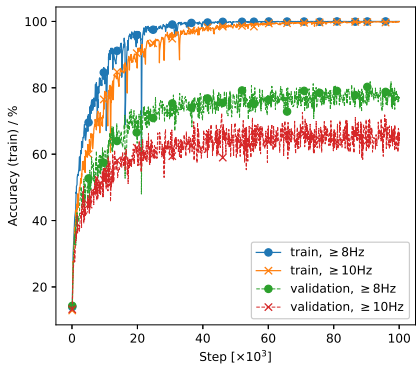

Figure 4: The validation accuracy when predicting low-frequency data by using high-frequency data of (≥ 8 [Hz]) and (≥ 10 [Hz]).

10 [Hz] data. As a comparison, Figure 5b show the 3 [Hz] data (orange) predicted by the deep learning model with both normalized raw data and beat tone data of high-frequency ($\geq$ 10 [Hz]). The proposed deep learning model successfully suppresses much of the high wavenumber information. Figure 6 compares the beat tone result and the deep learning prediction for 3 [Hz] on the same data set. However, since the source is moved away from the center, signals received far away from the source are difficult to tune. Leveraged by the data driven approach, the deep learning model demonstrates far more superior prediction performance in adapting to different scenarios

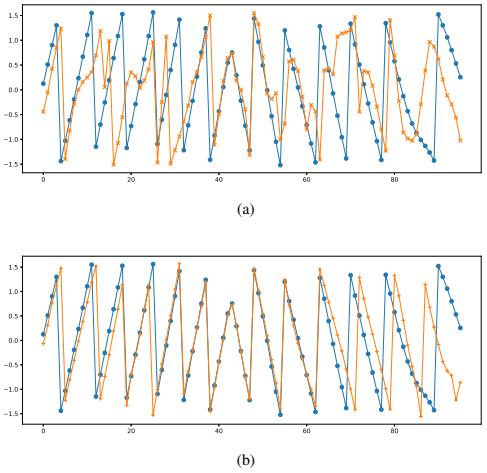

Figure 5: Source in the middle. (a) 3 [Hz] data (orange) predicted by the beat tone method. (b) 3 [Hz] data (orange) predicted by the deep learning model.

FWI Inversion

In this section, we compare the velocity model reconstructed by the FWI engine by using the 3 [Hz] data predicted by the

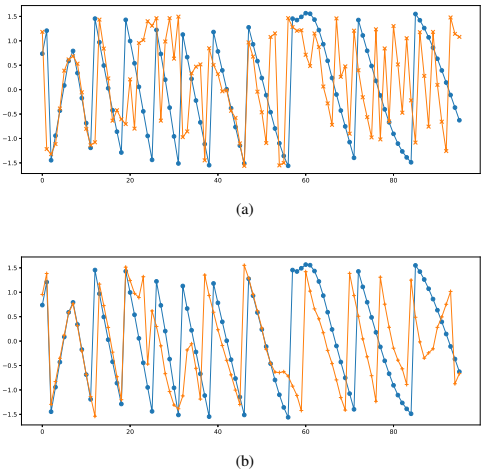

Figure 6: Source close to one side. (a) 3 [Hz] data (orange) predicted by the beat tone method. (b) 3 [Hz] data (orange) predicted by the deep learning model.

beat tone and our proposed deep learning model. The 3 [Hz] predicted the deep learning model is input into the *conventional* FWI engine for the inversion instead of the beat tone FWI engine used in Hu (2014). The starting model is a simple 1D linear model.

The FWI results of various scenarios are shown in Figure 7. Figure 7a shows the conventional FWI inversion result by using the true 3 [Hz] data. The beat tone FWI inversion result (beat tone 3 [Hz] data derived from 10 [Hz] and 13 [Hz] data) is shown in Figure 7b. The convention FWI inversion result of beat tone 3 [Hz] is displayed in Figure 7c. Although there is improvement by using the beat tone FWI inversion, high resolution artifacts are presented in Figure 7b due to scattering effects. When comparing Figure 7d, the conventional FWI inversion result of 3 [Hz] predicted from the high frequency data ($\geq$ 10 [Hz]) by the deep learning model, to Figure 7a, there is high level of similarity at the same spatial resolution.

Strong artifacts can be observed in Figure 7e if we perform the conventional FWI from 10 [Hz] directly using the 1D linear model. However, if we start the conventional FWI inversion of 10 [Hz] data by using Figure 7d as the initial model, we get a inversion result with much less artifacts. Figure 7h shows the conventional FWI inversion result implemented on the 10 [Hz], 11 [Hz], 12 [Hz], 13 [Hz] and [Hz] data sequentially after using Figure 7d. Similar patterns shown in Figure 7e, which is served as the reference solution, validate the quality of the predicated low-frequency data and the robustness of this deep learning model.

CONCLUSION

Starting the frequency continuation using the low-frequency data will help FWI to avoid convergence to local minima. However, it is a very challenging task to computationally synthesizing the low-frequency data from the high-frequency data. As the analytical solutions to the bandwidth extension problem often fail to adapt to different scenarios, we proposed a data driven approach leveraged by the deep learning network. The numerical example proves that the predicted low frequency data are very similar to the true low frequency data. By introducing more training models and training datasets with different varieties, the quality of the low frequency data prediction is expected to be significantly improved.

ACKNOWLEDGMENTS

This material is based upon work supported by National Science Foundation under Grant No. 1746824.

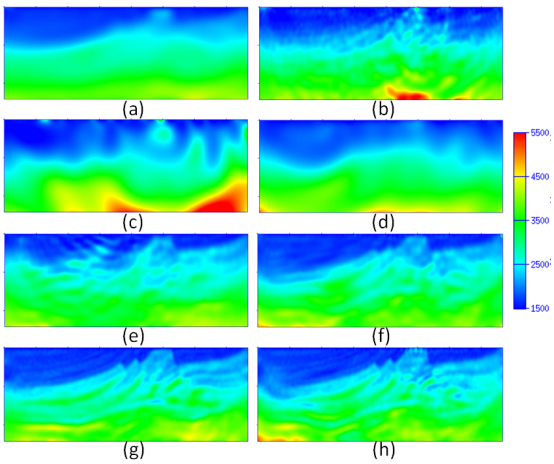

Figure 7: (a) True 3 [Hz] conventional FWI inversion; (b) 3 [Hz] beat tone FWI inversion (from 10 [Hz] and 13 [Hz]); (c) conventional FWI inversion with 3 [Hz] beat tone data (from 10 [Hz] and 13 [Hz]); (d) conventional FWI inversion with 3 [Hz] data predicted by the deep learning model ($\geq$ 10 [Hz]); (e) conventional FWI of 10 Hz data using 1D linear model as the starting model; (f) conventional FWI of 10 Hz data using the result d as the starting model; (e) reference solution of the conventional FWI using result a as the starting model and is implemented on the 6 [Hz], 10 [Hz], 12 [Hz], and 15 [Hz] data sequentially; (f) deep learning predicted 3Hz data (from data of $\geq$ 10 [Hz]) conventional FWI inversion , followed by 10 [Hz], 11 [Hz], 12 [Hz], 13 [Hz], and 15 [Hz] conventional FWI.

REFERENCES

Alkhalifah, T., 2014, Scattering-angle based filtering of the waveform inversion gradients: Geophysical Journal International, **200**, 363–373.

Baek, H., H. Calandra, and L. Demanet, 2014, Velocity estimation via registration-guided least-squares inversion: Geophysics, **79**, R79–R89.

Hu, W., 2014, Fwi without low frequency data-beat tone inversion: Presented at the 2014 SEG Annual Meeting, Society of Exploration Geophysicists.

Hu, W., J. Chen, L. Jianguo, and A. Abubakar, 2018, Retrieving low wavenumber information in fwi: IEEE Signal Processing Magazine, **35**, 132–141.

Li, Y. E., and L. Demanet, 2016, Full-waveform inversion with extrapolated low-frequency data: Geophysics, **81**, R339–R348.

Ma, Y., and D. Hale, 2013, Wave-equation reflection traveltime inversion with dynamic warping and full-waveform inversion: Geophysics, **78**, R223–R233.

Szegedy, C., S. Ioffe, V. Vanhoucke, and A. A. Alemi, 2017, Inception-v4, inception-resnet and the impact of residual connections on learning.: AAAI, 12.

Szegedy, C., W. Liu, Y. Jia, P. Sermanet, S. Reed, D. Anguelov, D. Erhan, V. Vanhoucke, A. Rabinovich, et al., 2015, Going deeper with convolutions: Presented at the , Cvpr.

Tang, Y., S. Lee, A. Baumstein, D. Hinkley, et al., 2013, Tomographically enhanced full wavefield inversion: Presented at the 2013 SEG Annual Meeting, Society of Exploration Geophysicists.

Van Leeuwen, T., and F. J. Herrmann, 2013, Mitigating local minima in full-waveform inversion by expanding the search space: Geophysical Journal International, **195**, 661–667.

Warner, M., and L. Guasch, 2016, Adaptive waveform inversion: Theory: Geophysics, **81**, R429–R445.